HIGH SCHOOL EDITION
Journal of Student Research
Volume 12 Issue 4 (2023)

Modelling Optical Invisibility in a Lenticular Microlens Array with Methods of Geometrical Optics and Weber's Contrast

Daniel Vorobiev

LETOVO School, USA

ABSTRACT

Though many advances have been made in exploring the 'cloaking' capabilities of metamaterials and optical systems in a wide range of the light spectrum, e.g. electromagnetic cloaking or paraxial ray optics, the phenomenon of unidirectional cloaking associated with 'woodpile' optical structures has not yet been widely discussed in the scope beyond experimental findings or digital integral cloaking; moreover, the relatively low cost of a lenticular array renders the investigation of its concealment properties in the visible regime of great interest for practical purposes. Thus, the following research paper provides an comprehensive theoretical model and analytical criterion for the phenomenon of unidirectional cloaking in the visible regime associated with a lenticular microlens array within the methods of computational ray optics (computing lens's spherical aberration using governing ray optics equations) and Weber's contrast (as perceived by the human eye) by considering the concealed object's virtual image as seen through a lenticular lens. Having shown that the criterion for practical invisibility adheres to our experimental results in determining the boundary case of invisibility, we employed it to explore the effect system parameters have on the array's cloaking capabilities. We established that the critical parameter for the array's cloaking capability is the diverging angle of an array's lenticular lens, the value of which positively correlates with the refraction index and the lens concave segment's curvature. Therefore, a lenticular array with most prominent cloaking capabilities consists of lenses with the greatest admissible index of refraction and a π arc measure for the lens's concave segment.

Introduction

A lenticular sheet, a.k.a. a lenticular microlens array is a transparent sheet that consists of an array of cylindrical plano-convex lenses arranged in a row, and often finds use in packaging and advertisements, where the technology of lenticular printing is used on packages or labels in order to create visual effects such as adding depth to the image, three dimensionality, the illusion of motion or the appearance of differing images seen through the lens depending on the angle at which the image is observed (1). According to Johnson and Barry (2), the active use of lenticular arrays for the purpose of visual effects began in the 1920's. In the same article the possibilities of lenticular arrays are further explored with the objective to develop a realistic analytical model and significantly improve image quality. A peculiar application of lenticular sheets is integral photography (the purpose of which is to allow users to see stereoscopic 3D images from arbitrary directions), where two perpendicularly placed lenticular sheets are used as a cheaper alternative to a "fish-eye" lens (3). Nowadays, lenticular arrays can also be found in art and specialized electronic displays.

An interesting property of a lenticular lens array, however, is not only its ability to create visual effects, but also to alter virtual images, concealing objects under certain conditions without the screening of their background and practically making the object invisible to the human eye in the visible regime (4) (see fig.1). The

research on lenticular lens cloaking capabilities is of current interest to science as the optical concealment applications range widely, from photography to urban design and architecture; meanwhile, the production cost for lenticular arrays is cheap when compared to more complex optical systems or metamaterials with similar cloaking capabilities.

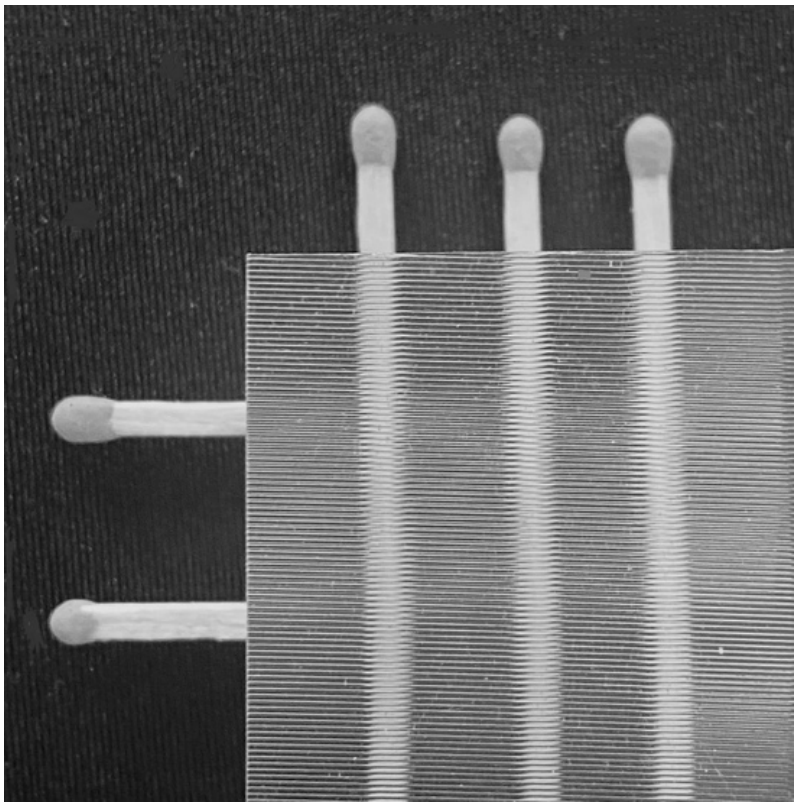

Figure 1. The effect of optical invisibility in a lenticular microlens array is demonstrated. Rows of lenticular lenses on the transparent lenticular sheet are arranged horizontally.

Overall, optical invisibility is an active research topic in physical optics: a holistic overview of advances in the field is provided by G. Gbur (5). For instance, in recent years, many findings in perfect invisibility have been made under transformation optics, where complex metamaterials have been shown to implement deformations in electromagnetic fields for the purposes of cloaking (6). Moreover, ray optics invisibility has also advanced significantly: Howell and Choi presented their approach to multidirectional object cloaking in the visible regime via axisymmetrical lenses (though the optical system grants a relatively small region available to cloaking) (7), as well as described active digital integral cloaking including an output lenticular lenslet array and employing digital displays for the purposes of simulating omnidirectional invisibility (8); Zhu, Lao, etc. experimentally demonstrated the cloaking effect for woodpile optical structures such as a lenticular array, and also discussed the cost-effective methods for 3D-printing of such optical systems (4). However, interestingly enough, the passive optical concealment capabilities of lenticular arrays, though unidirectional, have not been widely explored, nor, most importantly, has there been an analytical criterion for practical invisibility derived with consideration of the image's contrast perception by the human eye.

We hypothesized that the phenomenon of practical invisibility in the visible regime for a 'woodpile' optical array is not due to cloaking per se, but due to the strong diverging capabilities of a lenticular lens beyond its focal point, resulting in the object's virtual image distortion along one of its axis (fig.2B) and declining

perceived contrast with the background (meanwhile objects with noticeable width in the transverse section plane of the lens, in other words elongated objects placed perpendicular to the rows of lenticular lenses do not produce a distorted image. This is due to the fact that incident rays along the axis perpendicular to lens rows do not experience divergence). Therefore, in the scope of our research, we develop a novel criterion for cloaking based on Weber's contrast between the computed virtual image and object's background, which we then employed to explore how the cloaking capabilities of a lenticular microlens array depend on the diverging properties, particularly the diverging angle between extreme incident rays of lenticular lenses in the array.

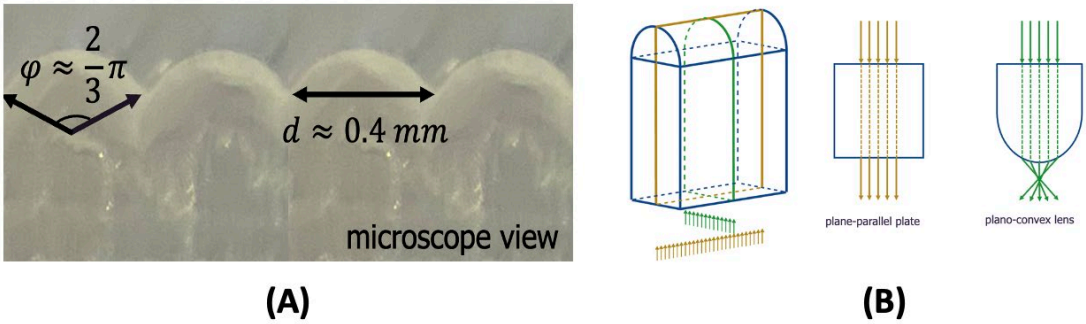

Figure 2.

(A) Transverse section of the lenticular microlens array (Axclear 70 LPI (ViPrint Clear Impact lens 70 Lpi) lenticular sheet) used in the boundary invisibility experiment as seen under the microscope with dimensions provided.

(B) We may consider the lenticular sheet to be a superposition of two optical systems - that of a plane-parallel plate and a lenticular lens outline. Rays along the first keep their trajectory, while those passing through the lens's transverse section strongly diverge.

Results

Single Lenticular Lens Spherical Aberration Modelling

Consider the lens's spherical aberration to be the virtual image of the object placed after the lenticular array – a justifiable proposition if the lens's size is negligible when compared with the object dimensions. By applying Snell's law of refraction (13) and considering system parameters including R (radius of curvature of the lenticular lens's convex segment), n (lens's refraction index), H (the height of the lens's convex segment), W (the horizontal width of a lenticular lens in its transverse section), D (distance from the lens to the object/screen), we aim to find the final coordinate X_{exit} of the point of intersection between the refracted light and the screen axis relative to the symmetry axis of the lens, as well as the angle at which the light has left the lens f_{exit}, depending on X_{in}, the initial incident ray coordinates relative to the lens's symmetry axis. The range of values for X_{in} is determined solely by the width, W, of the lenticular microlens. We have acquired a system of governing equations for the spherical aberration of a lenticular lens within ray optics (see fig.3). For the sake of simplifying computation, we have rewritten the ray transfer matrices (14) into algebraic notation.

(1) $\sin\alpha = n \cdot sin\beta$, Snell's law of refraction.

(2) $\frac{\sin(f_{exit})}{\sin(\alpha-\beta)} = n$, Snell's law for ray exiting the lens

$$(3)\quad \begin{cases} l = H - \sqrt{R^2 - \left(\frac{W}{2}\right)^2} \\ \sin\alpha = X_{in}/R \\ Y = R\sqrt{1-\sin^2\alpha} \\ X_{exit} = \frac{l}{\cot(\alpha-\beta)} - X_{in} \end{cases}, \text{ geometrical ratios}$$

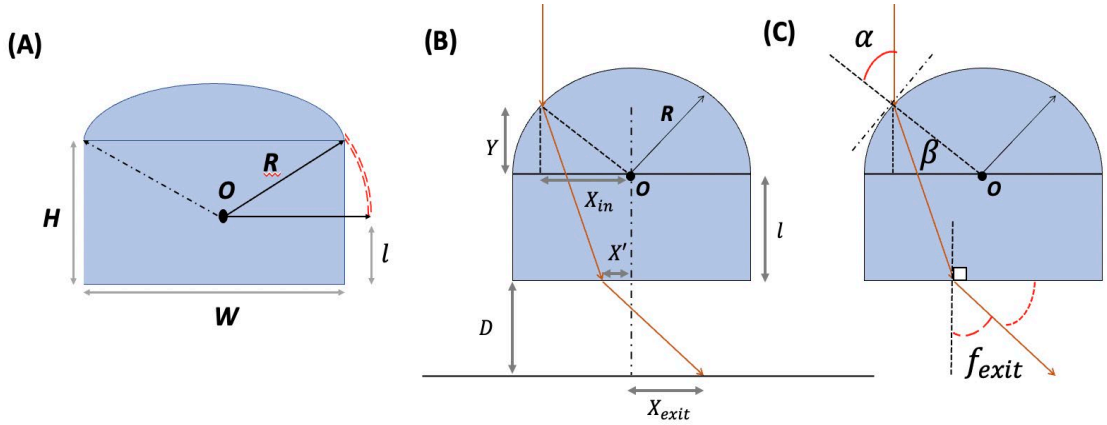

Figure 3. (A) – transverse schematic of a lenticular lens; Ray refraction trajectories: (B) - metric, (C) – angular

Thus, the lens's aberration and ray incident trajectories are computed based on these equations (fig. 4). Moreover, the coordinate of the critical ray liable to full internal reflection was acquired: $X_{1cr} \rightarrow R$. The methods and corresponding governing equations for modelling a bottom-oriented lenticular lens spherical aberration are identical to those of top orientation:

$$(4)\quad \begin{cases} \sin(f) = n \cdot \cos\alpha, \ Snell's\ Law \\ \cos\alpha = X_{in}/R \\ X_{exit} = X_{in} - \tan(f-\alpha)\,(D - \sqrt{X_{in}^2 - R^2}) \end{cases},$$

where f is the angle at which the incident ray has left the lens (relative to the normal) and $Y1$ is the distance from the top of the lens to the screen. Solving the system for a set of X_{in} coordinates (lying in the range of W, the lens's horizontal width), we retrieve the lens's spherical aberration. Moreover, it has been derived that the initial coordinate of the critical ray liable to full internal refraction is $X_{cr} \rightarrow \frac{2}{3}R$.

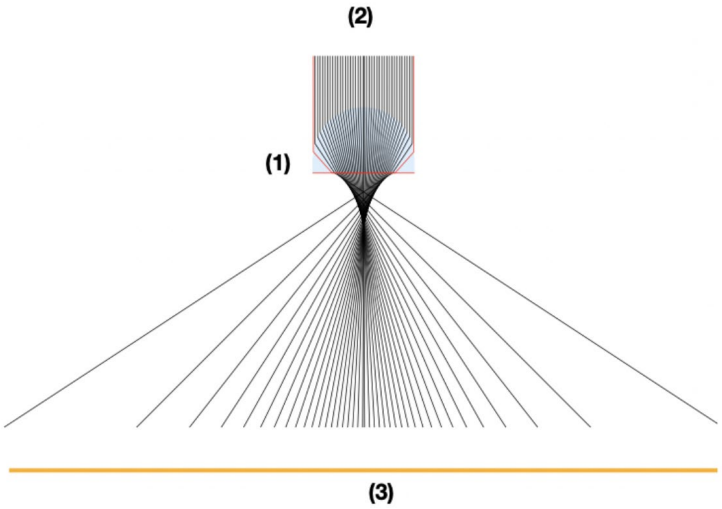

Figure 4. Computer simulation of spherical aberration through a lenticular lens past the focal point represented graphically. (1)– lenticular lens; (2) – distant observer; (3) - screen plane. The light rays liable to total internal reflection are marked in red. Computed in Wolfram Mathematica software.

Criterion for Lenticular Lens Practical Invisibility in The Visible Regime

The lens's spherical aberration may be represented via a distribution function dependent on the coordinate relative to the symmetry axis of the lenticular lens. For these purposes, the Cauchy distribution was fitted via the Least Squares Fit method (Fig. 5).

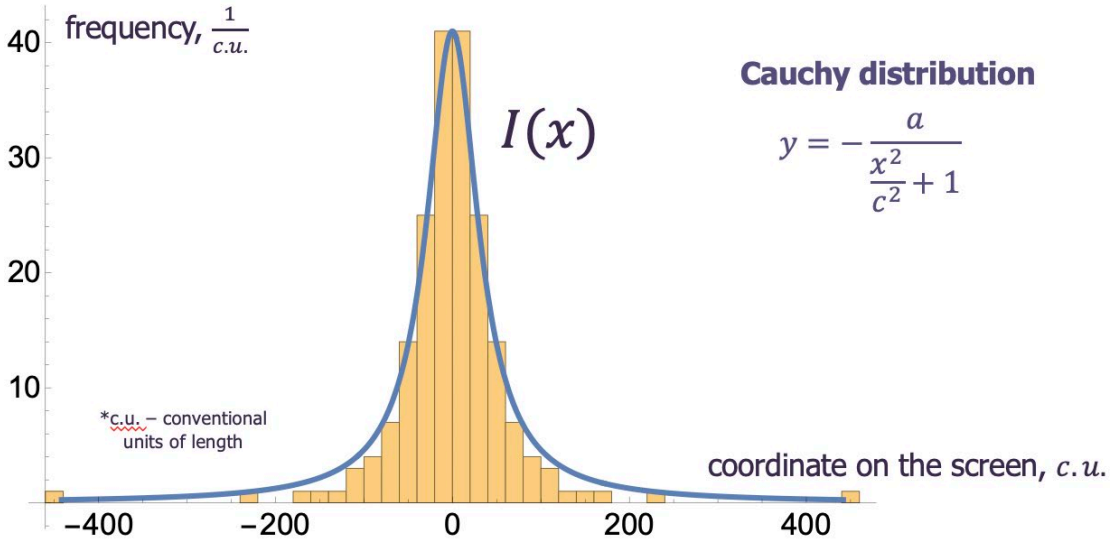

Figure 5. Cauchy distribution function fitted to ray distribution histogram of on-screen rays retrieved from the computed model of the lenticular lens's spherical aberration.

$$(5) \quad f(x) = b - \frac{a}{\frac{x^2}{c^2}+1} \quad \text{Cauchy Distribution}$$

Knowing the I(x) ray distribution function, in other words, the intensity distribution for a lenticular lens (determined by inputted system parameters) and the coordinates of an object's particular transverse section on the screen, we can determine the ratio of the light rays reflected off the object to the rays reflected off the object's background (the screen) for the object's image by integrating the intensity distribution.

$$(6)\quad \Phi = \frac{\int_{x1}^{x2} I(x)dx}{\int_{-x_{max}}^{x_{max}} I(x)dx - \int_{x1}^{x2} I(x)dx}$$

where $X1$ and $X2$ are the coordinates of the object on screen relative to the lens symmetry axis, x_{max} and $-x_{max}$ are the on-screen coordinates of the two extreme light rays. As stated in the hypothesis, the effect of optical invisibility is believed to be due to the contrast between the object's image and background tending to the contrast threshold value (M) - the minimum contrast value distinguishable by the human eye (M = 0.02). Therefore, we must first determine the brightness of the object's image when discussing invisibility, as, according to Weber-Fechner's Law (9,10), the contrast coefficient between the object's image and its background is calculated via Weber's contrast. From the ray distribution function, I(x), we can express the brightness of the image, as it consists both of rays reflected from the screen and objects surfaces.

$$(7)\quad \mathrm{B_{img}} = \frac{\mathrm{B_{obj}} \cdot \int_{x1}^{x2} I(x)dx + \mathrm{B_{backgr}} \cdot (\int_{-x_{max}}^{x_{max}} I(x)dx - \int_{-x1}^{x2} I(x)dx)}{\int_{-x_{max}}^{x_{max}} I(x)dx}$$

We may for convenience consider the coordinates of the object on the screen axis to be $-l$ and l in order for it to be symmetric relative to the symmetry axis of the lens - such a simplification is based upon the fact that there will often be a lens on the lenticular sheet for which the shared symmetry of the object and the single lens itself will hold true (due to the negligibly small dimensions of a single lens when compared to the object size or the value of distance from the screen).

$$(8)\ \mathrm{B_{img}} = \mathrm{B_{obj}} \cdot \int_{-l}^{l} I(x) + \mathrm{B_{backgr}} \cdot (1 - \int_{-l}^{l} I(x))$$

$$(9)\ \text{Weber's Contrast: } K = \frac{B_{obj} - B_{backgr}}{B_{backgr}},$$

where B_{obj}, B_{backgr} are the corresponding object and image brightness values.

Applying this to Weber's contrast formula and simplifying the expression the condition of optical invisibility for a lenticular lens array is described by the following analytical inequality:

$$(10)\ \int_{-l}^{l} \mathrm{I(x)dx} \cdot \frac{|\mathrm{B_{backgr}} - \mathrm{B_{obj}}|}{\mathrm{B_{backgr}}} \leq M$$

Boundary Cloaking Experiment

We aimed to test the cloaking criterion for the boundary case of invisibility via experiment. The perceived optical invisibility behind a lenticular sheet occurs when the contrast value (Weber's contrast) between the object's background and the object's image through the lens drops below the empirical minimum threshold value for the human eye. Thus, for our experimental setup (see fig.8), we placed an object of variable width, such as a filled triangle outline, behind the lenticular sheet in order to determine the extreme case of optical invisibility by considering the object's maximum width liable to concealment due to Weber's contrast criteria (9,10) while varying the independent variable of the distance betwen the lenticular sheet and object.

Using computer image processing software (see 'Methods'), we registered the point along the triangle's median where the image's contrast with the background is equal to the contrast threshold value, and, thus, determined the maximum width liable to optical concealment dependent on the distance between the lenticular sheet and the object (see fig.6)

In order to confirm the derived invisibility criteria (formula 10) by comparing it with the boundary invisibility experiment (see 'Results'), we considered the criteria's extreme case (boundary condition for practical invisibility):

$$(11)\ \int_{-l}^{l} \mathrm{I(x)dx} \cdot \frac{|\mathrm{B_{backgr}} - \mathrm{B_{obj}}|}{\mathrm{B_{backgr}}} = M$$

To determine the I(x) function, we computed the spherical aberration for the lens used in the experiment – the lens's geometrical and optical parameters as input parameters, as well as the initial contrast between the object (dark triangle) and background (light screen), were assessed beforehand (see *'Materials and Methods'*). Thus, we computed the dependency of the maximum object width liable to concealment, $2I_{max}$, on the distance between the object and the lenticular sheet, H, and compared it to the boundary invisibility experiment (see fig.6).

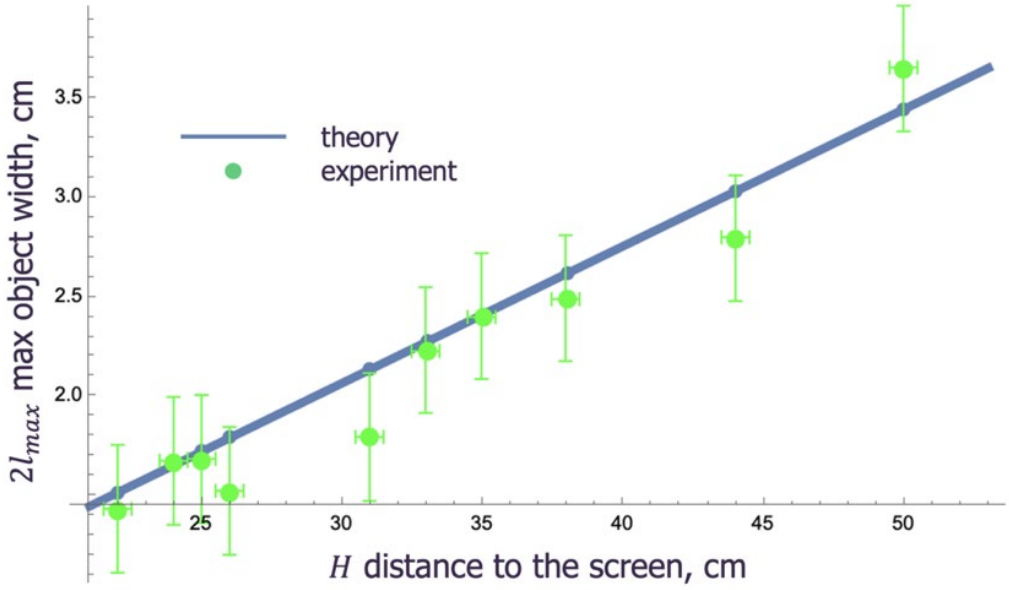

Figure 6. Experimental value of the maximum width, *Wmax*, of an object liable to optical concealment behind a lenticular sheet compared with the theoretical value of $2I_{max}$ (see *'Discussion'*) dependent on the distance between the object and the lenticular sheet. Results of the boundary case invisibility experiment: dependency of the maximum object width liable to optical concealment on the distance.

Effect of Lens's Diverging Properties On an Array's Cloaking Capabilities

In the scope of the hypothesis, we investigated how the cloaking capabilities of the array depend on the diverging properties of a single lenticular lens. For this, a link was made between the theoretical boundary cloaking criterion (which we derived in previous sections) and the lens's optical properties.

The growth of the value $\int_{-l}^{l} \mathrm{I(x)}\, dx$, the integral intensity distribution, in correlation with value of l, we defined as the function $Int(l)$. As $(\frac{\mathrm{B_{backgr}} - \mathrm{B_{obj}}}{\mathrm{B_{backgr}}})$, the initial contrast, is an experimentally determined constant, if aiming to maximize l and meet the invisibility concealment criteria, we must minimise the rate of growth of the function $Int(l)$. Therefore, when comparing the optical concealment properties of lenses, the corresponding $Int(l)$ functions are compared. Consider the asymptotic case of $Int(l)$ with 1 being the asymptote, expressing $Int(l)$ in terms of the Cauchy distribution parameters.

$$\int \mathrm{I(x)dx} = \int -\frac{\mathrm{a}}{\frac{x^2}{\mathrm{c}^2} + 1}\, \mathrm{dx} = -\mathrm{ac} \cdot \arctan\left(\frac{x}{c}\right) + C)$$

$$\mathrm{Int(l)} = -2\mathrm{ac} \cdot \arctan(\frac{\mathrm{l}}{\mathrm{c}})$$

The function's asymptote has the value of 1 with one of the parameters being equal to 2/pi:

$$(\mathbf{12}) \quad \mathrm{Int(l)} = \frac{2}{\pi} \cdot \arctan(\frac{\mathrm{l}}{\mathrm{c}})$$

Hence c is the only parameter of $Int(l)$, meaning that all $Int(l)$ functions for our ray distribution are of the same shape, but reach the extremum of 1 at different coordinates. $Int(l)$ corresponds to the growth of the definite integral of the $I(x)$ ray distribution function for different l values, the object's dimensions. From the extreme case of the invisibility criteria we know that the definite integral is equal to a constant. The object's coordinate, then, corresponds to the point of intersection between $Int(l)$ and the previously mentioned constant, l is the abscissa coordinate of such a point. To maximize array's cloaking capabilities, the l object coordinate must be maximized. Hence, the function $Int(l)$ must be extended along the abscissa. With this, the normalized $Int(l)$ function's rate of growth, and, therefore, the value of l_{max}, with all other parameters pre-set, is defined by and is proportional in direct correlation to the range value of the lens (the on-screen distance between the two extreme incident rays after refraction). The lens's range in itself is dependent on the distance and the diverging angle of the lens. But the distance is variable, hence the diverging angle of a lens is the critical parameter for the cloaking criterion and, thus, cloaking capabilities of a lenticular array. If two lenticular lenses are compared and their spherical aberration image may be approximated with Cauchy distribution, the one with the greater divergence angle will conceal an object of greater size with all other system parameters fixed. Moreover, we derived the formula for the divergence angle value in terms of lens parameters:

$$(13) \quad \gamma = 2 \cdot \arcsin\left(\frac{Wn}{2R}\left(\sqrt{1 - (\frac{d}{2WR})^2} - \frac{\sqrt{1 - \frac{W^2}{2R}}}{n}\right)\right)$$

where W is the horizontal lens width in the transverse section, n - lens material refraction index, R - convex segment curvature radius. The two graphs (fig. 7) represent the dependence of the diverging angle value, which has been determined to be the lens effectiveness parameter, on the values of the refraction index of the lens and the relation between the width of the lens and the diameter of the convex segment. Hence, we concluded that the most capable lenticular lens in terms of optical concealment hosts a π arc measure of the convex segment, highest admissible refraction index, and the convex segment facing the distant observer.

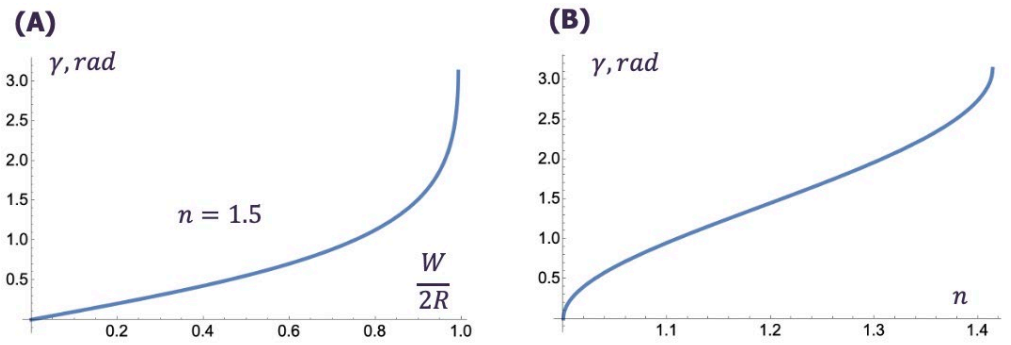

Figure 7.

(A) - The diverging angle on the relation of width to radius theoretical dependence, $\gamma(\frac{W}{2R})$, with n=1.5;

(B) - the diverging angle on the refraction coefficient theoretical dependence, $\gamma(n)$, with $\frac{W}{2R} = 1$.

Discussion

In order to investigate the key hypothesis further in the study, we first developed a novel quantitative criterion for lenticular array cloaking in the visible regime dependent on system parameters by considering Weber's contrast (9,10) as perceived by the human eye between an object's computed virtual image through a single lenticular lens and the object's background. For the purposes of computing the virtual image of an object placed after the lenticular array, an auxiliary hypothesis was made that the single microlens's spherical aberration is to be considered the object's virtual image as seen by a distant observer – a justifiable proposition if the lens's dimensions are negligible compared to those of the object. The presented inequality (formula 10) is the decisive criteria for optical concealment of an object, as in itself the theoretical invisibility criteria contains a variety of system parameters, such as the initial contrast between the object and its background ($\frac{B_{backgr} - B_{obj}}{B_{backgr}}$), the dimensions of the object liable to concealment, l and $-l$ (the extreme coordinates of the object's transverse section), the distance between the lens and the screen and the lens's parameters contained in $I(x)$, the computed intensity distribution function, as well as the value of the human eye contrast threshold M, an experimentally determined constant.

Having shown that the derived criterion for cloaking adheres to the experimental results in determining the boundary case of optical invisibility via contrast image processing techniques, we employed the model to test our research's hypothesis and show that the critical parameter for the array's cloaking capability is indeed the diverging angle of an array's lenticular lens. In turn, the value of the diverging angle specific to a lenticular lens positively correlates, as shown in our study, with the array's refraction index and the lens concave segment's curvature; therefore, a lenticular array with the most prominent cloaking capabilities consists of lenses with the greatest admissible index of refraction and a π arc measure for the lens's concave segment, as this grants the greatest angle of divergence.

We must discuss the limitations of the model and, correspondingly, cloaking criterion. It is to be noted that in reality the virtual image of the object perceived by the observer's eye consists of rays from multiple neighboring lenses. Let us consider the computed intensity distribution for three rows of lenticular lenses - the model can be evaluated by performing parallel transferring each of the refracted ray by the value of $2W$, where W is the lens width. The normalized $Int(I)$ functions for both cases reach the maximum value of 1 at the corresponding $r/2$ coordinates (r being the range of the lens), which for a single lens and three lenses differs by only $2W$ - a value negligible enough when considering the entire range of a lens. The range for K lenses is,

similarly, by $(K-1)\cdot \mathrm{W}$. We may then compile a formula for the error of a single lens virtual image compared to an array:

$$(15)\ \mathrm{E} = \left(\frac{(\mathrm{k}-1)\cdot \mathrm{W}}{\mathrm{r}+(\mathrm{k}-1)\cdot \mathrm{W}}\right)\cdot 100\%$$

k being the number of lenses, W - the width of the lens and r - range.

At $\mathrm{H} = 100\mathrm{cm}$ and R=0.01cm (the radius of the lens's convex segment) the error value is 4.3 %, Moreover, the function E(H), where H is the distance between the lens and the screen, is a decreasing function. Therefore, the difference error of a single lens simulation when compared to multiple lenses or a single lens is negligible enough at noticeable lens-to-screen distance for us to consider a single lens's spherical aberration and intensity distribution as an accurate substitution to an array.

In brief, our cloaking criteria may be used to predict the phenomena of practical invisibility in the visible regime after a lenticular lens array dependent on variable system and lens parameters, such as initial object-background contrast, distance, lens dimensions, and shape, as well as its optical properties. The testing of the key hypothesis regarding lens's the relation between diverging properties and the array's cloaking capabilities established that a lenticular array with the most prominent cloaking capabilities consists of lenses with the greatest admissible index of refraction and a π arc measure for the lens's concave segment.

In terms of future research, it would be beneficial to consider the effect of the observer's position, as well as interlaying of multiple arrays with the goal of achieving multidirectional cloaking. Practical invisibility associated with lenticular arrays, though unidirectional, can find various applications in displays, photography, design, and architecture, as well as being employed in urban infrastructure to conceal unappealing building sites, office buildings, if necessary, communication lines, etc.

Materials and Methods

Evaluation of Experimental Data

In the experiment with the boundary invisibility case (see *'Results'*) a dark equilateral triangle with a side length of 15 cm was placed behind an Axclear 70 LPI (ViPrint Clear Impact lens 70 Lpi) lenticular sheet (fig.1) on a light background (for experimental setup, see fig.8) and acted as the to-be-concealed object. A Canon EOS 300D camera with raw format for unaltered contrast values and 1-second exposure was used to take images of the object as seen through the lenticular sheet in a dimly-lit room with reduced light noise. Since the triangle has variable width along its height, the triangle's image through the lenticular lens was processed along the median of the triangle, from the top pixel and down, acquiring the mean value of image brightness for 5 pixels adjacent to the pixel situated on the triangle's median dependant on triangle width in the corresponding point. We linearised the pixel brightness data set (fig. 8, C), and thus were able to determine the boundary case of invisibility by considering the contrast between the image and background as the contrast threshold value for the human eye, K = 0.02 (11). As it is known how the width relates to the vertical coordinate of the triangle, we registered the maximum width liable to optical concealment dependent on the distance between the lenticular sheet and the object.

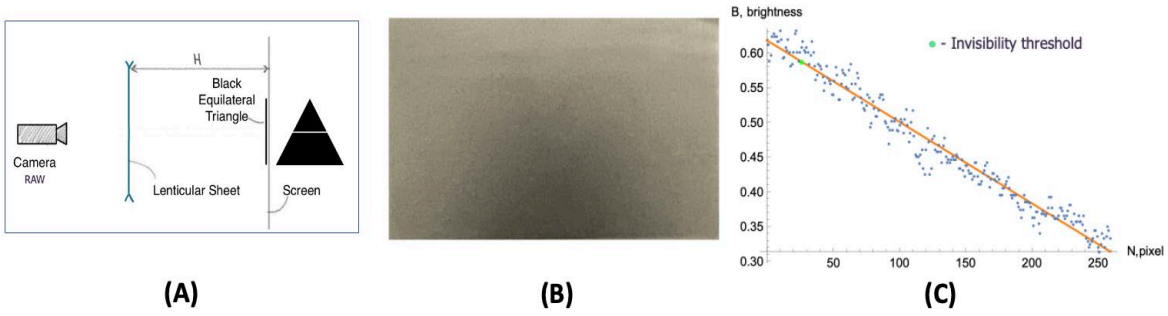

Figure 8.

(A)- A dark equilateral triangle with a side length of 15 cm was placed behind an Axclear 70 LPI (ViPrint Clear Impact lens 70 Lpi) lenticular sheet (fig.1). A Canon EOS 300D camera with raw format for unaltered contrast values and 1-second exposure was used to take images of the object as seen through the lenticular sheet in a dimly-lit room with reduced light noise.

(B)– Image of the black triangle as seen through the lenticular sheet.

(C)- Dependency of the brightness of the image pixel on the number of the pixel along the triangle's median; point of contrast threshold with the background was calculated via the linearization of image brightness data set

Computer Simulation

Wolfram Mathematica software was employed for the purposes of computing spherical lens aberration and the $I(x)$ distribution function for the invisibility criteria and was also used to process brightness and contrast of images (see *'Results'*). Tracker software was employed to determine the arc shape of the lenticular lens used in the experiment to input it into the model. The spherical aberration model takes the system parameters (R - radius of curvature of the lenticular lens's convex segment, n - lens's refraction index, H - the height of the lens's convex segment, W - the horizontal width of a lenticular lens in its transverse section, D - distance from the lens to the object/screen) as an input and outputs the $I(x)$ ray distribution function needed in the theoretical invisibility criteria, which also considers the initial contrast between the object and its background. The lens's geometrical parameters are determined by applying Tracker software to the image of the lens's transverse section under the microscope (fig. 1). The refraction index n is determined by applying the Fresnel equations to Brewster's angle formula. These values are determined using a laser, pointed at the horizontally placed lens at an angle, and a piece of polarized glass detecting the reflected ray. The average refraction index value of the lenticular sheet used later on in experiments was $n = 1.6$. The result is in fact accurate considering that the lenticular array used in the experiments was made of PET (Polyethylene terephthalate).

Acknowledgments

Special thanks to Letovo IYPT team for all the help and support.

References

(1) Niemuth, Todd R. *Plastic Sheets with Lenticular Lens Array*. 20 Aug. 2009, patents.google.com/patent/US8411363B2/en.

(2) Johnson, R. Barry, and Gary A. Jacobsen. "Advances in Lenticular Lens Arrays for Visual

Display." *Current Developments in Lens Design and Optical Engineering VI*, 18 Aug. 2005, doi.org/10.1117/12.618082.
(3) Yanaka, Kazuhisa. "Integral Photography Suitable for Small-Lot Production Using Mutually Perpendicular Lenticular Sheets and Fractional View." *Stereoscopic Displays and Virtual Reality Systems XIV*, 15 Feb. 2007, doi.org/10.1117/12.704393.
(4) Zhu, Jian, et al. "3D-Printed Woodpile Structure for Integral Imaging and Invisibility Cloaking." *Materials & Design*, vol. 191, June 2020, p. 108618, doi.org/10.1016/j.matdes.2020.108618.
(5) Gbur, Greg. "Invisibility Physics: Past, Present, and Future." *Elsevier EBooks*, 1 Jan. 2013, pp. 65–114, doi.org/10.1016/b978-0-444-62644-8.00002-9.
(6) McCall, Martin. "Transformation Optics and Cloaking." *Contemporary Physics*, vol. 54, no. 6, Nov. 2013, pp. 273–286, doi.org/10.1080/00107514.2013.847678.
(7) Choi, Joseph S., and John C. Howell. "Paraxial Ray Optics Cloaking." *Optics Express*, vol. 22, no. 24, 18 Nov. 2014, p. 29465, doi.org/10.1364/oe.22.029465.
(8) Choi, Joseph S., and John C. Howell. "Digital Integral Cloaking." *Optica*, vol. 3, no. 5, 19 May 2016, p. 536, doi.org/10.1364/optica.3.000536
(9) Peli, Eli. "Contrast in Complex Images." *Journal of the Optical Society of America A*, vol. 7, no. 10, 1 Oct. 1990, p. 2032, doi.org/10.1364/josaa.7.002032.
(10) Portugal, R. D., and B. F. Svaiter. "Weber-Fechner Law and the Optimality of the Logarithmic Scale." *Minds and Machines*, vol. 21, no. 1, 29 Dec. 2010, pp. 73–81, doi.org/10.1007/s11023-010-9221-z.
(11) "Contrast Threshold - International Dictionary of Marine Aids to Navigation." *Www.iala-Aism.org*, www.iala-aism.org/wiki/dictionary/index.php/Contrast_Threshold.
(12) M. Born, E. Wolf. *Principles of Optics*. Cambridge, Cambridge University Press, 2019.
(13) Yu N., Patrice Genevet, et al. "Light Propagation with Phase Discontinuities: Generalized Laws of Reflection and Refraction." *Science*, vol. 334, no. 6054, 1 Sept. 2011, pp. 333–337, science.sciencemag.org/content/334/6054/333/tab-pdf, doi.org/10.1126/science.1210713.
(14) Smith, Warren J. *Modern Optical Engineering, 4th Ed.* McGraw Hill Professional, 25 Dec. 2007.